

Whole-Body Angular Momentum Estimation Using Reduced-Order Models

Nicholas Hale
Clemson University
Clemson, United States
nahale@clemson.edu

Miao Yu
Clemson University
Clemson, United States
myu2@clemson.edu

Reed Gurchiek
Clemson University
Clemson, United States
rgurchi@clemson.edu

Ge Lv
Clemson University
Clemson, United States
glv@clemson.edu

Abstract—Whole-body angular momentum is commonly used to quantify balance control. However, its computation typically requires full-body segment kinematics, increasing experimental and computational burden. We evaluate four reduced-order body-segment models for estimating WBAM and a model-defined center of mass: NoArms (removes both arms), NoTop (removes arms and torso), ConTor (welds the arms to the torso as a single segment using a frozen arms-at-side posture), and ConPel (condenses the mass of the pelvis, torso, and arms into a point mass at the pelvis). Model estimates are compared against full-body WBAM during level walking. In the sagittal plane, NoArms provided the closest match (an NRMSD of 1.16 percent and a correlation coefficient of 0.9998). In the transverse plane, all reduced models showed large magnitude errors; ConTor performed best (an NRMSD of 71.0 percent and a correlation coefficient of 0.9673). In the frontal plane, ConTor again performed best (an NRMSD of 3.25 percent and a correlation coefficient of 0.9967). Correlations remained high overall (a minimum correlation coefficient of 0.9042), indicating that several reduced models preserve gross waveform timing despite amplitude bias. These results support reduced-order WBAM estimation when qualitative trends are sufficient and highlight limitations in transverse-plane analyses where arm dynamics are critical.

Index Terms—OpenSim, Whole-Body Angular Momentum

I. INTRODUCTION

In biomechanics research, whole-body angular momentum (WBAM) is the net angular momentum of the human body resulting from the translations and rotations of body segments about the system’s center of mass (CoM). WBAM is a key biomechanical indicator commonly used to quantify and interpret an individual’s balance-control strategies during both reciprocating and perturbed locomotion [1], as well as during other functional tasks [2]–[4]. During walking, the neuromuscular system modulates WBAM and limits net angular momentum, in part through inter-segmental cancellation among the limbs and trunk [5]. Because impaired stability during walking and related motor tasks increases fall risk and injury likelihood, and is related to broader adverse health outcomes [6], [7], WBAM provides a principled metric for characterizing an individual’s capacity to regulate dynamic balance [2]–[4]. Actively altering WBAM via powered exoskeletons has also been shown to be effective in reducing muscular effort across a wide range of locomotor tasks [8], [9], further demonstrating its potential in quantifying human performance.

While it is an important metric, WBAM is often calculated from human joint kinematics sampled by motion capture systems and/or inertial measurement units (IMUs) for each body segment. This process typically requires a complex setup of motion capture systems, and a full-body kinematic model of a human can require 50 sensors. Motion capture cameras can also lose line of sight on markers, causing errors and gaps in the data [10]. Due to the difficulty of real-time WBAM estimation, some exoskeleton balance controllers employ reduced WBAM estimates in their design [8], [9], [11]. Therefore, it would be beneficial to propose and analyze reduced-order human models for estimating WBAM with fewer resource investments and computational costs.

Prior studies have explored the development and validation of reduced-order models. In [12], the authors quantified the rotational and translational contributions of individual body segments to sagittal-plane WBAM about the full system’s CoM. However, WBAM in the transverse and frontal planes was not considered, and all segmental contributions were referenced to the whole-body CoM. Estimating the whole-body CoM generally requires information from all body segments, including segments that may be excluded from a reduced-order WBAM computation. Reference [13] similarly investigated simplified WBAM modeling by merging the forearm and upper arm, the foot and shank, and the head and trunk, using subject-optimized fixed joint angles. Notably, their approach primarily reduces model complexity by merging segments rather than removing them.

In contrast, we construct four reduced-order models that include both a segment-merging approach (one model) and segment-removal approaches (three models) in the sagittal, transverse, and frontal planes, with WBAM computed about a model-specific CoM defined only by the segments retained in each model. We present these models and evaluate their WBAM estimates by comparing them against full-body WBAM.

The remainder of the paper is organized as follows. Sec. II describes the dataset, analysis tools, reduced-order models, the procedure to calculate normalized WBAM, and the two metrics used to compare reduced-order estimates with the full-body WBAM reference. Sec. III presents plane-specific results for each subject and summarizes the findings across the sagittal, transverse, and frontal planes. Finally, Sec. IV

discusses study limitations and outlines directions for possible future work.

II. METHODS

A. Dataset

We analyzed data from a publicly available Gait120 dataset [14] using the `OpenSim` API (version 4.5) [15] and `MATLAB` R2025a [16]. Of the 120 subjects from the dataset [14], subjects with code 001, 002, 004, 005, and 007 were used for analysis. Each subject completed two steady-state walking strides per trial across five trials, yielding 10 strides per subject. A stride was defined as the interval from left heel strike to the subsequent left heel strike. Subjects 003 and 006 were excluded because only 1 stride was recorded per trial, yielding 5 total strides for each subject. The demographics and average walking speeds of the subjects are shown in Table I.

TABLE I
SUBJECT DEMOGRAPHICS AND THEIR AVERAGE WALKING SPEED OVER 10 STEADY-STATE STRIDES (MEAN \pm STANDARD DEVIATION)

Subject	Age	Sex	Height (m)	Mass (kg)	Speed (m/s)
001	20	Male	1.64	48.2	1.35 \pm 0.03
002	24	Male	1.76	85.0	1.22 \pm 0.05
004	23	Male	1.69	64.0	1.52 \pm 0.04
005	20	Male	1.75	67.5	1.20 \pm 0.02
007	24	Male	1.74	57.1	1.28 \pm 0.03

B. Reduced-Order Models

We considered five models, including four with reduced or modified body segments and one full-body model with all original segments (Fig. 1).

The model with all original body segments (hereafter referred to as the Full model) consists of the left-right pairs of the femur, tibia, patella, talus, calcaneus, toes, humerus, ulna, radius, and hand, in addition to the torso and pelvis. The model used in this report is based on the Rajagopal `OpenSim` full-body model [17], with the head and torso merged into a single torso segment as defined in the Gait120 dataset [14]. The first reduced-order model is a 14-segment model with the humerus, ulna, radius, and hand removed, and is defined as the NoArms model. The second reduced-order model is a 13-segment model with both arms and the torso removed, and is referred to as the NoTop model. The third reduced-order model has the same body segments as the Full model; however, the arms are assumed to always remain static at the side of the torso. Thus, their joint angles relative to the torso segment are locked, and the arms' inertial properties are combined with the torso. For this experiment, the frozen posture was defined as the first frame of each subject's first Stand-to-Sit trial in [14]. After rigidly fixing the arms to the torso, the model is reduced to 14 segments; we refer to this reduced representation as the ConTor (condensed torso) model. Finally, the last model has the same body segments as the NoTop model. In this 13-segment model, the pelvis is modeled as a

point mass that aggregates the arms' mass and the combined head-and-torso segment onto the pelvis's CoM. Consequently, the pelvis contributes no rotational component to WBAM.

C. Whole-Body Angular Momentum Calculation

The WBAM for each model was calculated following the method in [18] as:

$$\vec{H}_j = \sum_{i=1}^n \left[(\vec{r}_s - \vec{r}_{b,i}) \times m_i (\vec{v}_s - \vec{v}_{b,i}) + I_i \vec{\omega}_i \right], \quad (1)$$

where \vec{H}_j is the WBAM vector of reduced-order model j with $j \in \{\text{NoArms, NoTop, ConTor, ConPel}\}$, \vec{r}_s is the combined CoM position of the entire model, $\vec{r}_{b,i}$ is the CoM position of body segment i , m_i is the mass of body segment i , \vec{v}_s is the entire model's CoM velocity vector, $\vec{v}_{b,i}$ is the CoM velocity of body i , I_i is the inertia matrix of body i , and $\vec{\omega}_i$ is the angular velocity of body i . The CoM values were computed for each model individually using the model's reduced segment count. We normalized WBAM to produce a unitless quantity by multiplication with the scalar N given as [19]:

$$N = \frac{1}{L m_s \sqrt{gL}}, \quad (2)$$

with L as the height of the subject, m_s the mass of the subject, and g the acceleration due to gravity. All WBAM values used in this paper have been normalized by this method.

D. Metrics for Comparison

Each reduced-order model was compared with the full model using two methods: normalized root-mean-square difference (NRMSD) and the correlation coefficient. The NRMSD between \vec{H}_j and the WBAM of the full model \vec{H}_F is given as:

$$\text{NRMSD}_j^n (\%) = 100 \cdot \frac{\sqrt{\frac{1}{V} \sum_{k=1}^V [H_j^n(k) - H_F^n(k)]^2}}{\max_{1 \leq k \leq V} |H_F^n(k)|}, \quad (3)$$

where V is the total number of WBAM frames, k indexes each frame, and $n \in \{\text{Sagittal, Transverse, Frontal}\}$ denotes the plane of interest. This metric quantifies the root-mean-square deviation between a reduced-order model and the Full model, normalized by the peak absolute Full-model WBAM in the corresponding plane. Lower NRMSD values, therefore, indicate closer agreement in WBAM magnitude, whereas larger values indicate greater deviation from the Full-model reference. An NRMSD of 100% indicates that the root-mean-square estimation error is equal to the peak absolute WBAM magnitude of the Full model in that plane.

While NRMSD measures how well a series of data matches another series in magnitude and position, the correlation coefficient provides insight into how well one series' plot matches the shape of another [20]. The correlation coefficient was calculated using `MATLAB`'s `corr` function. `corr` uses Pearson's linear correlation coefficient ρ and is given as:

$$\rho_j^n = \frac{\sum_{k=1}^V \tilde{H}_j^n(k) \cdot \tilde{H}_F^n(k)}{\sqrt{\sum_{k=1}^V \tilde{H}_j^n(k)^2} \sqrt{\sum_{k=1}^V \tilde{H}_F^n(k)^2}}, \quad (4)$$

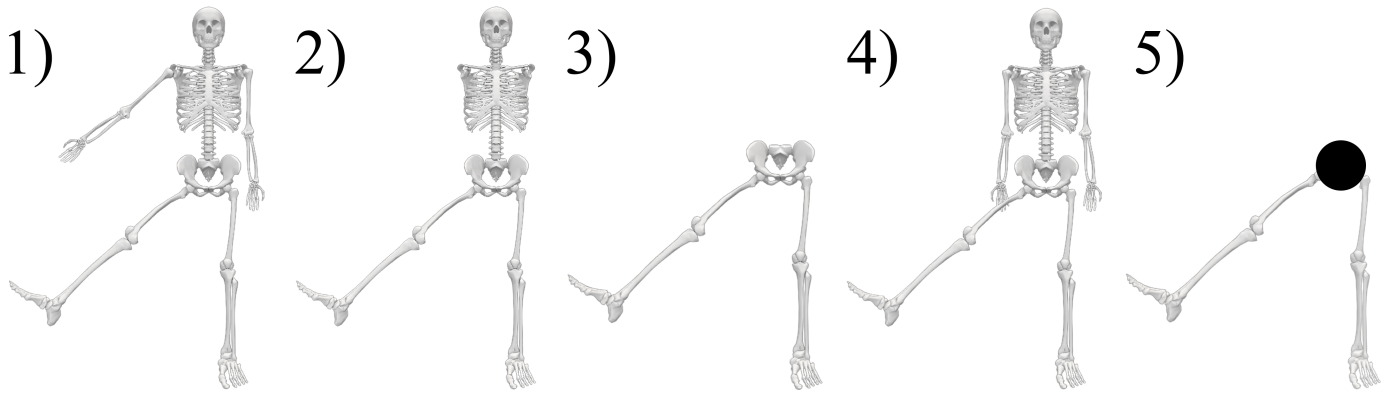


Fig. 1. The five models discussed in this experiment. From left to right: (1) Full model, (2) NoArms model, (3) NoTop model, (4) ConTor model, and (5) ConPel model.

where \tilde{H}_j^n is the demeaned WBAM of reduced model j in plane n , and \tilde{H}_F^n is the demeaned WBAM of the Full model in plane n . Demeaning is the process of subtracting the dataset’s mean from each point. The correlation coefficient uses demeaned values to focus on the shapes of the plots rather than their magnitudes, producing values between -1 and 1. Values closer to 1 represent a perfect imitation of the waveform shape, while values closer to -1 represent a perfectly inverted waveform.

Each stride was time-normalized to 0 – 100% stride using linear interpolation. NRMSD and ρ_j were computed separately for each stride and model, then averaged within subject and across subjects.

III. RESULTS AND DISCUSSION

A. Sagittal Plane

Fig. 2 shows the averaged WBAM estimations for each subject in the sagittal, transverse, and frontal planes. Across all subjects, the sagittal-plane plots show that the NoArms and ConTor models closely match the full model’s WBAM. The NoTop and ConPel models exhibit larger discrepancies, with the NoTop model generally underestimating and the ConPel model overestimating WBAM. For subjects 002, 004, and 007, the ConPel model also reaches the first peak earlier than the others.

Table II shows the mean NRMSD and correlation coefficients across all subjects in the sagittal plane. The NoArms model outperforms the ConTor model, though the difference is minor (less than 1%). Their correlation coefficients are also both high and very close, with the NoArms model being slightly better. This minuscule difference highlights the limited impact of the arms on estimating sagittal-plane WBAM. Overall, the NoArms model is preferable because it avoids the need to estimate the arms’ resting moments of inertia and their contributions to the torso CoM while also yielding better performance.

Table II shows that the simpler models struggle more than the NoArms and ConTor models, with the NoTop and ConPel models each showing approximately 10% error relative to the

TABLE II
SAGITTAL-PLANE MEAN PERFORMANCE ACROSS ALL SUBJECTS.

Model Type	NRMSD (%)	Correlation
NoArms	1.163	0.9998
NoTop	10.506	0.9813
ConTor	1.920	0.9992
ConPel	9.499	0.9893

Full model. The ConPel model is slightly better at matching the Full model’s WBAM magnitude, but the difference is only about 1%. The approximately 9% difference highlights the significance of the combined torso-and-head segment on the Full model’s WBAM magnitude. However, the torso segment seems to have a reduced effect on matching the shape of the Full WBAM plots, as the NoTop and ConPel models have correlation coefficients of 0.9813 and 0.9893, respectively.

These results indicate that these models can serve different sagittal-plane use cases depending on the study objective. If accurate WBAM magnitude and waveform fidelity relative to the Full model are required, the arms may be omitted during data collection (NoArms). If only the overall waveform shape is needed, the ConPel model offers a further reduction in segment count. However, users should account for its tendency to produce slightly earlier peaks than the Full model.

B. Transverse Plane

The transverse plane shows substantially worse results. All models, across each subject, show substantial separation from the Full model. Each reduced-order model overestimates the Full WBAM, and none include the swinging motion of the arms during the gait cycle, highlighting the substantial impact of the arms on WBAM generation in the transverse plane. Since the WBAM of the Full model is lower than that of the reduced-order models, the arms must contribute to lowering WBAM and thereby increasing stability. An important observation is that, in the transverse plane, the overall waveform of the Full model’s WBAM is reasonably captured by the NoArms and ConTor models. Although these two models tend to exaggerate the amplitudes of peaks, troughs, and inflection

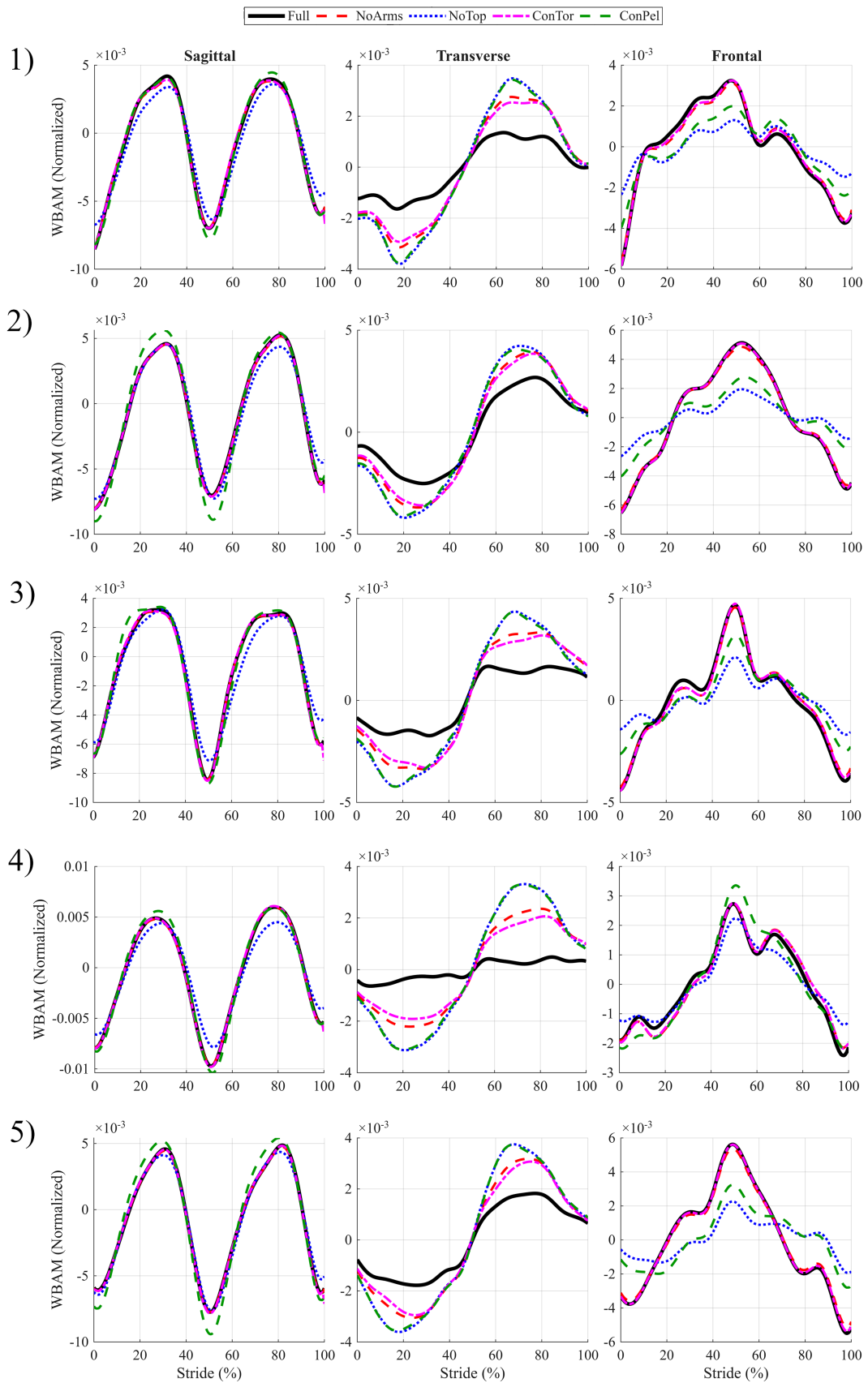


Fig. 2. WBAM plots in the sagittal, transverse, and frontal planes. From top to bottom: Subjects 001, 002, 004, 005, and 007. In this paper, forward motion is defined along the $-Z$ axis, and the Y axis points vertically upward.

points, the timing of these features largely aligns with the Full model’s trace. In contrast, the NoTop and ConPel models are less consistent in reproducing the Full model’s waveform and exhibit larger, more persistent errors than the NoArms and ConTor models.

Table III reinforces the conclusion drawn from the plots. All NRMSD values are very high, indicating that each proposed reduced-order model deviates substantially from the Full model’s actual WBAM values. While the ConTor model is 10 percentage points lower than the NoArms model, its error remains high at approximately 71% NRMSD. The NoTop and ConPel models differ by less than 2%, and both exceed 100%. Together, these results indicate that each model approximately doubles the WBAM magnitude of the Full model.

TABLE III
TRANSVERSE-PLANE MEAN PERFORMANCE ACROSS ALL SUBJECTS.

Model Type	NRMSD (%)	Correlation
NoArms	81.812	0.9636
NoTop	111.858	0.9440
ConTor	70.951	0.9673
ConPel	109.312	0.9427

The higher correlation values support the observation from the plots that the NoArms and ConTor models capture the overall transverse-plane WBAM waveform, even though they do not match its magnitude. Correlations of approximately 0.96–0.97 still indicate meaningful shape error, and the enormous magnitude discrepancies further limit their utility. These models are therefore only suitable when a study requires a coarse characterization of waveform shape and can tolerate both amplitude bias and residual shape mismatch. In contrast, the NoTop and ConPel models perform worse and, together with their large NRMSD values, are not appropriate for transverse-plane analyses. Because arm motions strongly influence transverse-plane WBAM, the loss of arm contributions in reduced-order models is likely not an acceptable trade-off in most biomechanics applications.

C. Frontal Plane

The frontal-plane WBAM estimations in Fig. 2 show that the NoArms and ConTor models appear to overlap the Full model’s WBAM very well. The NoTop and ConPel models consistently underestimate the Full model’s WBAM, except for Subject 004, where the ConPel model appears to overestimate WBAM. Visually, each reduced-order model appears to estimate the shape of the Full model’s WBAM well, with similar peaks and troughs occurring at the same points in the gait cycle.

Table IV supports the claims made by visual analysis of the plots. The NoArms and ConTor models each have NRMSD values below 5% and very high correlation coefficients ($\rho > 0.99$). These models estimate the waveform shape well and exhibit only modest magnitude errors. In contrast, the NoTop and ConPel models perform poorly in both magnitude

TABLE IV
FRONTAL-PLANE MEAN PERFORMANCE ACROSS ALL SUBJECTS.

Model Type	NRMSD (%)	Correlation
NoArms	4.538	0.9959
NoTop	29.462	0.9042
ConTor	3.253	0.9967
ConPel	23.021	0.9318

and shape, both exceeding 20% error relative to the full-body WBAM. Their correlation coefficients below 0.94 further indicate limited ability to reproduce the full-body waveform.

In the frontal plane, the NoArms and ConTor models closely match the WBAM of the Full model, whereas NoTop and ConPel show substantial errors in both waveform shape and magnitude. These results underscore the importance of the combined torso-and-head segment in generating frontal-plane WBAM. Accordingly, for frontal-plane WBAM estimation, the ConTor model is the preferred representation based on these data.

Overall, the ConTor model performs best across all three planes. It has the best performance metrics in the transverse and frontal planes, and ranks second in the sagittal plane. While it is only slightly worse in NRMSD in the sagittal plane than the NoArms model, the ConTor model is 10 percentage points lower than the next-best model in the transverse plane and 1 percentage point lower in the frontal plane. The ConTor model is therefore the best general model if one must be chosen without regard to the specific niche each model fills.

IV. LIMITATIONS AND FUTURE WORK

The presented WBAM comparisons among reduced-order models are limited to five non-disabled subjects performing level-ground walking at self-selected speeds, with a relatively small number of steady-state strides per subject (10 strides). As a result, the reported NRMSD and correlation should be interpreted as task- and data-specific, and may not directly generalize to other locomotor tasks or clinical populations.

Going forward, the ConTor model should be refined by improving the definition of the “arms-at-the-side” posture. In the current implementation, the arms are frozen at the first frame of a stand-to-sit trial, which may not reflect a natural arms-at-rest configuration during gait. A more defensible approach would define the frozen arm posture using either the gait phase at which the arms most closely approximate a neutral, side-hanging position (e.g., minimal shoulder/elbow angular velocity) or dedicated static calibration trials in which the subjects stand naturally with their arms at their sides. Future work should also evaluate the performance of these proposed reduced-order models across a wide range of locomotor tasks, such as stair ascent/descent, turning, and perturbed walking, to determine how well the results generalize.

Finally, walking speeds should be explicitly controlled. Inter-subject differences in speed and trial-to-trial variability may introduce additional confounds that can affect WBAM magnitude and timing.

V. CONCLUSION

This paper demonstrates that reduced-order models can provide useful WBAM estimates in the sagittal and frontal planes during walking. In the sagittal plane, the NoArms model performed the best and closely matched the Full model's WBAM values. If only a coarse representation of the WBAM shape is needed, the ConPel model could be acceptable despite its 9.5% NRMSD. In the frontal plane, the ConTor model showed strong performance with approximately 3% NRMSD and a high correlation coefficient. Reduced-order models without the torso segment are not recommended, as the NoTop and ConPel models exhibited substantial errors in both the magnitude and shape of WBAM. No reduced-order model is recommended for transverse-plane WBAM estimation. Without considering explicit arm dynamics, all proposed models failed to capture the correct magnitude or shape. At best, the ConTor model may provide a qualitative approximation of transverse-plane waveform timing with a trade-off in magnitude accuracy.

ACKNOWLEDGMENT

The authors thank Professor Seungbum Koo at the Korea Advanced Institute of Science and Technology for providing the essential OpenSim files.

REFERENCES

- [1] S. Shokouhi, P. Sritharan, and P. V.-S. Lee, "Recovering whole-body angular momentum and margin of stability after treadmill-induced perturbations during sloped walking in healthy young adults," *Sci. Rep.*, vol. 14, no. 1, p. 4421, 2024.
- [2] G. C. Simoneau and D. E. Krebs, "Whole-body momentum during gait: A preliminary study of non-fallers and frequent fallers," *Journal of Applied Biomechanics*, vol. 16, no. 1, pp. 1–13, Feb. 2000.
- [3] M. D. Adam, D. McElvain, T. G. Hornby, A. S. Hyngstrom, and B. D. Schmit, "Whole body angular momentum characterizes reactive balance adaptations and perturbation intensity," *J. Biomech.*, vol. 179, p. 112474, Jan. 2025.
- [4] B. K. Kaya, D. E. Krebs, and P. O. Riley, "Dynamic stability in elders: momentum control in locomotor adl," *The Journals of Gerontology Series A: Biological Sciences and Medical Sciences*, vol. 53, no. 2, pp. M126–M134, Mar. 1998.
- [5] L. Z. Rubenstein and K. R. Josephson, "The epidemiology of falls and syncope," *Clinics in Geriatric Medicine*, vol. 18, no. 2, pp. 141–158, 2002.
- [6] B. Salzman, "Gait and balance disorders in older adults," *American Family Physician*, vol. 82, no. 1, pp. 61–68, Jul. 2010.
- [7] A. K. Silverman and R. R. Neptune, "Differences in whole-body angular momentum between below-knee amputees and non-amputees across walking speeds," *J. Biomech.*, vol. 44, no. 3, pp. 379–385, Feb. 2011.
- [8] M. Yu and G. Lv, "Task-invariant centroidal momentum shaping for lower-limb exoskeletons," in *IEEE 61st Conference on Decision and Control (CDC)*, 2022, pp. 2054–2060.
- [9] M. Yu, J. Dean, and G. Lv, "Centroidal momentum shaping for task-agnostic assistance: Theory and validations on a bilateral hip exoskeleton," *IEEE Rob. Autom. Lett.*, 2026, to appear.
- [10] B. R. Hindle, J. W. L. Keogh, and A. V. Lorimer, "Inertial-based human motion capture: A technical summary of current processing methodologies for spatiotemporal and kinematic measures," *Appl. Bionics Biomech.*, p. 6628320, Mar. 2021.
- [11] A. Vallinas Prieto, A. Q. L. Keemink, E. H. F. van Asseldonk, and H. van der Kooij, "Implementation and tuning of momentum-based controller for standing balance in a lower-limb exoskeleton with paraplegic user," *IEEE Trans. Neural Syst. Rehabil. Eng.*, vol. 33, pp. 343–353, 2025.
- [12] J. Zhang, M. van Mierlo, P. H. Veltink, and E. H. F. van Asseldonk, "Estimation of sagittal-plane whole-body angular momentum during perturbed and unperturbed gait using simplified body models," *Hum. Mov. Sci.*, vol. 93, p. 103179, Feb. 2024.
- [13] M. Liu, A. Naseri, I.-C. Lee, X. Hu, M. D. Lewek, and H. Huang, "A simplified model for whole-body angular momentum calculation," *Med. Eng. Phys.*, vol. 111, p. 103944, Jan. 2023.
- [14] J. Boo, D. Seo, M. Kim, and S. Koo, "Comprehensive human locomotion and electromyography dataset: Gait120," *Sci. Data*, vol. 12, no. 1, Jun. 2025.
- [15] SimTK, "Opensim: Project home," simtk.org, accessed: 2026-01-23. [Online]. Available: <https://simtk.org/projects/opensim/>
- [16] The MathWorks Inc., "Matlab," MathWorks, version R2025a. Accessed: 2026-05-14. [Online]. Available: <https://www.mathworks.com/products/matlab.html>
- [17] A. Rajagopal, C. L. Dembia, M. S. DeMers, D. D. Delp, J. L. Hicks, and S. L. Delp, "Full-body musculoskeletal model for muscle-driven simulation of human gait," *IEEE Trans. Biomed. Eng.*, vol. 63, no. 10, pp. 2068–2079, Oct. 2016.
- [18] A. K. Silverman, J. M. Wilken, E. H. Sinitiski, and R. R. Neptune, "Whole-body angular momentum in incline and decline walking," *J. Biomech.*, vol. 45, no. 6, pp. 965–971, Apr. 2012.
- [19] N. G. Gomez, J. A. Dunn, M. A. Gomez, and K. B. Foreman, "The effect of amplitude normalization technique, walking speed, and reporting metric on whole-body angular momentum and its interpretation during normal gait," *J. Biomech.*, vol. 168, p. 112075, May 2024.
- [20] D. D. Molinaro, I. Kang, and A. J. Young, "Estimating human joint moments using exoskeleton control, reducing user effort," *Sci. Rob.*, vol. 9, no. 88, p. eadi8852, 2024.